The Solvation of Mg^{2+} with Gas-Phase Clusters Composed of Alcohol Molecules

Bohan Wu, Bridgette J. Duncombe,† and Anthony J. Stace*

Department of Physical Chemistry, School of Chemistry, The University of Nottingham, University Park, Nottingham NG7 2RD, United Kingdom

Received: October 26, 2007; In Final Form: December 20, 2007

The dication Mg^{2+} has been clustered with a range of different alcohols to form $[Mg(ROH)_N]^{2+}$ complexes, where N lies in the range 2−10. Observations on the chemistry of the complexes reveal two separate patterns of behavior: (i) unimolecular metastable decay, where at small values of N the complexes undergo rapid charge separation via Coulomb explosion; and (ii) electron capture-induced decay, where collisional activation promotes bond-breaking processes via charge reduction. For the latter it has been possible to identify a generic set of reactions that are common to all of the different $[Mg(ROH)_N]^{2+}$ complexes; however, there are examples of reactions that are specific to individual alcohols and values of N. For metastable decay, it is shown that there is a clear correlation between the value of N at which a complex ceases to be metastable and the ionization energy of R, the radical that forms the complementary ion in the Coulomb explosion step. Metastable decay in two of the $[Mg(ROH)_N]^{2+}$ complexes follows a very different pathway that eventually results in proton abstraction. It is suggested that this difference is due to the precursor complexes adopting geometries that have at least one ROH molecule in a secondary solvation shell.

Introduction

In recent years there have been considerable advances in the techniques available for generating and studying the chemical and spectroscopic properties of metal dication complexes in the gas phase.[1−3] Between the two prominent experimental methods for preparing complexes, electrospray[2] and pick-up,[1] the array of ligands accessible to gas-phase experiments ranges from the rare gases[4] to bulky substituted di- and triethylamines.[2] Despite this high level of activity, little experimental information exists on the behavior of metal dications in association with ligands that constitute a homologous series.[2] In principle, such a series should provide one of the few opportunities to explore changes in metal ion stability and solvation that may occur as a result of a systematic variation in one or more molecular properties. Examples of such variations could include size (steric effects), polarizability, and dipole moment. Presented here are results from an extensive series of experiments that have investigated the behavior of dication complexes consisting of Mg^{2+} in association with clusters composed of methanol, ethanol, *n*-propanol, *n*-butanol, and *t*-butanol. Observed chemical processes include metastable Coulomb explosion and $H^{\cdot}$ and $R^{\cdot}$ loss promoted by electron capture. Although there are systematic patterns of behavior within the range of systems studied, the results reveal significant variations in the abilities of the different alcohols to form stable (as opposed to metastable) solvate units.

Mg^{2+} in association with methanol clusters has been the subject of two studies, one by Woodward et al.[5] and the other by Kohler and Leary.[6] Both studies examined the collision-induced chemistry of $[Mg(CH_3OH)_N]^{2+}$ complexes, which showed a variety of neutral loss and charge-transfer reactions, the latter mostly in the form of proton transfer. Kohler and Leary also studied Mn^{2+} and Co^{2+} with methanol and observed a variety of reactions, including hydride and proton transfer, and ligand cleavage.[6] The photochemistry of Co^{2+}/methanol clusters has been studied by Thompson et al.[7] where the dominant reaction pathway is again proton transfer. Two other studies have reported data on the interaction of Mg^{2+} with higher alcohols:[8,9] one was limited to relative intensity measurements, and the other gave preliminary results on charge separation (Coulomb explosion) in Mg^{2+}/propanol clusters. Propanol has also been studied in association with Sr^{2+}, where reactions very similar to those seen for the corresponding Mg^{2+} complexes were observed.[10]

In contrast to the lack of experimental data on Mg^{2+}/alcohol clusters, there have been numerous studies devoted to the equivalent singly charged species. Ohashi and co-workers[11] have examined the solvation structures of $Mg^+(CH_3OH)_N$ clusters ($N = 1-4$) using infrared photodissociation spectroscopy and density functional theory. Their results show that, for complexes larger than $Mg^+(CH_3OH)_3$, stable structures consist of a mixture of isomers where molecules either coordinate directly to the metal cation, or they form structures that consist of three methanol molecules bound directly to the metal ion and a fourth ligand occupying an outer shell via hydrogen bonding.[11] These conclusions are supported by calculations undertaken by Lu and Yang.[12] In both studies, the number of methanol molecules bonded to the metal ion in the first solvation shell appears to be limited to three by ligand−ligand repulsion.[11,12] However, the structures of $[Mg(CH_3OH)_N]^{2+}$ cluster ions may not necessarily be the same as those of $[Mg(CH_3OH)_N]^+$ clusters as, apart from the difference in charge, electron repulsion from the partially filled 3s orbital of Mg^+ will also have an influence on geometry. Cabaleiro-Lago and Rodriguez-Otero have calculated the geometries of $M^+(CH_3OH)_N$ clusters, where M = K, Rb, Cs (isoelectronic with alkaline earth metal M^{2+} ions) and $N = 3$ and 4.[13] In addition to primary shell structures, they also found stable surface structures, in which the methanol molecules are all located on one side of the metal ion and bound by a network

* Corresponding author. E-mail: anthony.stace@nottingham.ac.uk.
† Present address: School of Chemistry, University of Edinburgh, The King's Buildings, West Mains Road, Edinburgh EH9 3JJ, UK.

10.1021/jp710369x CCC: $40.75 © 2008 American Chemical Society
Published on Web 02/15/2008

of hydrogen bonds.[13] Although the charge on the metal cation may be different, some of the experimental results reported here for Mg^{2+}/alcohol clusters can be identified with several of the geometric configurations calculated for $Mg^{+}(CH_3OH)_N$ clusters. In particular, there are examples of where hydrogen-bonded structures are proposed as means of facilitating proton transfer.

Experimental Section

The experimental apparatus used for generation, identification, and detection of gas-phase multiply charged metal−ligand complexes has been described extensively in previous publications.[8,14] Briefly, mixed neutral clusters were produced by the adiabatic expansion of a gas mixture consisting of alcohol entrained with argon through a pulsed supersonic nozzle. Such a mixture was generated by flowing argon through a reservoir holding a sample of the alcohol and then adjusting the temperature of the latter (usually with ice) to achieve optimum signal intensity. Neutral clusters of varying composition including Ar_M, $Ar_M(ROH)_N$, and $(ROH)_N$ then passed through a region where magnesium vapor ($\sim 10^{-2}$ mbar) was generated by a Knudsen effusion cell (DCA Instruments, EC-40-63-21) operating at 470 °C. The neutral magnesium atoms collided with the cluster beam to produce mixed neutral clusters thought to be of the form $MgAr_M(ROH)_N$. Because the beam consists of a wide range of mixed clusters, a shutter at the exit to the oven is used to confirm the presence of magnesium in signals by noting the difference in intensity between the shutter being open and closed. As there are three Mg isotopes (^{24}Mg = 78.99%, ^{25}Mg = 10.00%, ^{26}Mg = 11.01%), comparisons could also be made between precursor ions with different *m*/*z* values.

Neutral clusters, some of which contain a single metal atom, entered the ion source of a high-resolution reverse geometry double focusing mass spectrometer (VG-ZAB-E), where they were subjected to high-energy electron ionization (∼70−100 eV). Because only ions rather than neutral complexes were detected in these experiments, it is likely that extensive ligand evaporation takes place, which presumably helps to reduce the internal energy content of complexes. Accordingly, under most experimental conditions no ion complexes of the form $[Mg(Ar)_M(ROH)_N]^{z+}$ were detected.

Mass analyzed kinetic energy spectroscopy (MIKES)[15] has been employed extensively to analyze the stability and chemical reactivity of ions from the series $[Mg(ROH)_N]^{2+}$. Ions with a specific *m*/*z* value were selected using a magnet, and the products of their decay were then identified as they passed through an electrostatic analyzer (ESA).[15] Such measurements provide evidence of the fragmentation pathways adopted by an ion of a certain size that, in turn, can often be used to infer details of structure. The MIKES technique can be used to study both unimolecular (metastable) decay and processes induced by collision activation. A collision cell located between the magnet and the ESA allows ions to enter and exit, while keeping the escape of collision gas to a minimum. Gas was introduced into the cell via a needle valve, and sufficient amount was added to reduce the precursor ion intensity by ∼50%. A wide range of charge reduction and fragmentation pathways can be activated in this way, and the gases used included He, N_2, O_2, and Xe. The vacuum in the flight tube as a whole does not change significantly, as differential pumping is located close to the cell.

To provide accurate differentiation between processes taking place within the collision cell and those occurring elsewhere within the flight tube, a voltage can be applied to the cell. Under normal circumstances, the laboratory-frame kinetic energy of a fragment ion, E_f, can be calculated from the following expression:

$$E_f = \frac{m_f\, q_p}{m_p q_f} E_p \tag{1}$$

where m_f and m_p are the masses of the fragment and precursor ions, respectively, and q_f and q_p are their charges. With the addition of a voltage, V_c, to the collision cell, a separate, collision-induced signal can be detected at a kinetic energy E_{fc}, which is given by the expression:

$$E_{fc} = \frac{m_f\, q_p}{m_p q_f} E_p + \frac{m_p q_f - m_f\, q_p}{m_p q_f} V_c \tag{2}$$

The precise voltage applied to the cell was calibrated using the collision-induced reactions of CO_2^{2+}.

The MIKES technique has been used to study two types of unimolecular (metastable) fragmentation that take place in the absence of collisions and where fragmentation relies on the presence of residual internal energy remaining after electron ionization. As will be seen, sufficient energy remained to promote two separate pathways: (i) charge separation (Coulomb explosion) in small complexes; and (ii) neutral molecule loss in larger complexes. As compared to our earlier experiments on $[Mg(ROH)_N]^{2+}$ complexes,[5,9] the data presented here have been recorded under conditions where there has been a significant improvement in energy resolution and sensitivity. As a result, it is now possible to distinguish unambiguously between fragmentation pathways that differ by ±1 amu. In the past, our inability to make this assignment has caused problems with interpretation.

Results

Within the data acquired from these experiments there are generic results that typify behavior exhibited by a majority of the $[Mg(ROH)_N]^{2+}$ complexes, and these results are summarized here. Using either nitrogen or oxygen as the collision gas (Cg), evidence for a majority of the following reactions can be found within complexes involving each of the different alcohols.

$$[Mg(ROH)_N]^{2+} + Cg \rightarrow [Mg(ROH)_{N-K}]^{2+} + K\mathrm{ROH} + Cg \tag{3}$$

$$[Mg(ROH)_N]^{2+} + Cg \rightarrow Mg^{+}(ROH)_N + Cg^{+} \tag{4}$$

$$[Mg(ROH)_N]^{2+} + Cg \rightarrow Mg^{+}(ROH)_{N-K} + K\mathrm{ROH} + Cg^{+} \tag{5}$$

$$[Mg(ROH)_N]^{2+} + Cg \rightarrow MgOH^{+}(ROH)_{N-K-1} + K\mathrm{ROH} + R + Cg^{+} \tag{6}$$

$$[Mg(ROH)_N]^{2+} + Cg \rightarrow MgOR^{+}(ROH)_{N-K-1} + K\mathrm{ROH} + H + Cg^{+} \tag{7}$$

Several of the singly charged metal-containing products have previously been identified in an earlier study of $[Mg(CH_3OH)_N]^{2+}$ complexes involving collision-induced dissociation.[5] However, earlier interpretations of charge reduction in protic solvents had assumed all reactions proceeded via intracomplex charge transfer, with proton transfer being the dominant mechanism. Instead, many of the fragment ions now appear to

have unexpectedly narrow kinetic energy spreads (see below), which do not equate with charge separation followed by Coulomb explosion. In addition, our own experiments show a marked absence of counterions, for example, R^+ as opposed to $R^{\cdot}$ in reaction 6 above, which can be accounted for by assuming electron capture is the charge reduction mechanism. This revised interpretation of events has come about through improvements in sensitivity and resolution,[16,17] which make it possible to distinguish between reaction steps 5 and 7, where the difference is a single H atom. This also means that a number of new reaction pathways have been identified.

At the laboratory-frame ion kinetic energies involved in these experiments (10 000 eV), electron capture on the part of metal dications appears to be a very efficient charge reduction process with a comparatively high collision cross section (~20 Å),[18] which contrasts with the 1−2 Å cross section for collisional activation.[15] Although it was expected that electron capture, as represented by steps 4−7, made a contribution to the observed level of charge reduction, the extent was not fully recognized until a recent high-resolution study of $[Mg(NH_3)_N]^{2+}$ complexes.[16] Depending on the nature of the collision gas, considerable variation has been observed in the efficiency of electron capture, with xenon proving to be the most effective gas, closely followed by O_2 and N_2.[16] In addition to reactions 3−7, further examples of electron capture-induced dissociation (ECID) that appear to be specific to certain complexes will be identified below in MIKES scans presented for size-selected $[Mg(ROH)_N]^{2+}$ ions. Metastable decay also appears to show significant variation according to either the size or the composition of a complex, and specific examples of this behavior will also be discussed below.

An analysis of the fragmentation patterns of the complexes reveals that, of the two principal products, $MgOR^+(ROH)_M$ (reaction 7) and $Mg^+(ROH)_M$ (reaction 5), the former gradually increases in intensity as a function of *N*. In the case of methanol, the switch from $Mg^+(CH_3OH)_M$ to $MgOCH_3^+(CH_3OH)_M$ was noted in an earlier study where both sets of ion intensities were recorded directly, and there it was found that $MgOCH_3^+(CH_3OH)_M$ becomes the dominant ion when $N \geq 4$.[5] What this present study confirms is that the observed pattern arises as a consequence of competing reaction pathways. Similar behavior is seen here for all of the alcohols examined in this study; however, it has not been possible to quantify the trend, only to state that the $MgOR^+(ROH)_M$ ion becomes the dominant fragment in larger complexes. The observation of a switch in reaction products is similar to that recorded by Fuke and co-workers in their experiments on singly charged alkaline-earth metal ions with water clusters.[19,20] They reported two ion series, $M^+(H_2O)_N$ and $MOH^+(H_2O)_{N-1}$ (M = Mg and Ca). $MOH^+(H_2O)_{N-1}$ ions were found to be produced via an H-atom elimination reaction, and they were exclusively observed for $6 \leq N \leq 14$ in the mass spectra. The switch at $N = 5$ was ascribed to a difference in the successive hydration energies of M^+ and MOH^+, with the latter being more stable in the presence of large numbers of water molecules.[19,20]

One final feature of the results that is common to all of the complexes is the observation that the dications with maximum intensity have the composition $[Mg(ROH)_4]^{2+}$, and that when reaction 3 occurs (the loss of neutral methanol) the tendency is for complexes where $N > 4$ to show preferential fragmention down to $N = 4$. These observations confirm results on selected alcohol complexes from previous experiments[8] and are also supported by measurements undertaken using all three magnesium isotopes.[21]

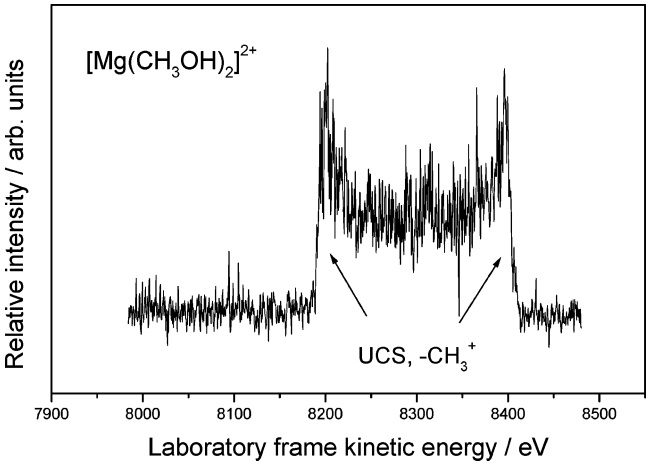

Figure 1. Kinetic energy profile recorded following the metastable unimolecular decay of $[Mg(CH_3OH)_2]^{2+}$ to produce $MgOH^+CH_3OH + CH_3^+$. The peak shape is indicative of Coulomb explosion.

(A) Mg^{2+}/Methanol Complexes. The smallest $[Mg(CH_3OH)_N]^{2+}$ complex observed was $[Mg(CH_3OH)_2]^{2+}$, which suggests that $N = 1$ may be unstable under the experimental conditions used in this work. Assuming no other factors contribute to the stability of this complex, the total energy required to stabilize the cluster ion will be the difference between the ionization energies of Mg^+ (15.0 eV) and CH_3OH (10.84 eV); hence, each ligand stabilizes the complex by 2.08 eV. As evidence of the metastability of $[Mg(CH_3OH)_2]^{2+}$, Figure 1 shows a fragment peak recorded from a MIKES scan taken at a base pressure ~5×10^{-8} mbar in the flight tube and where the product $MgOH^+CH_3OH$ arises from the unimolecular charge separation (UCS) reaction:

$$[Mg(CH_3OH)_2]^{2+} \rightarrow MgOH^+CH_3OH + CH_3^+ \qquad (8)$$

The dish-shaped peak is characteristic of the large release of kinetic energy that accompanies Coulomb repulsion.[15] The observation of this reaction as the only metastable process shows that charge transfer accompanied by the cleavage of a chemical bond within a ligand is more favorable than direct electron transfer from a ligand to the metal ion. In their study of collisions between metal dications and molecules, Tonkyn and Weisshaar proposed that in curve crossing processes, such as charge exchange, reactants follow the most exothermic process,[22] which in their case was H^- transfer as opposed to electron transfer. Similarly, density functional calculations on the unimolecular reactions of dihydrated alkaline earth metal dications have also shown that the proton-transfer products, MOH^+ and H_3O^+, are more favored than the charge-transfer products H_2O^+ and M^+H_2O.[23]

To provide a more quantitative analysis of the observed charge separation process, a one-dimensional potential energy curve model has been plotted in Figure 2 for the encounter between $Mg^{2+} + CH_3OH$. The positions of the curves have been determined through a combination of the exothermicities of the reactions involved and the ion−dipole and ion−induced dipole interactions that exist between Mg^{2+} and methanol.[8] Because the calculations only include one molecule, there is no curve corresponding to proton transfer as a reaction pathway (see below). Likewise, the influence additional molecules might have on the solvation (stabilization) of both the reactant dication and the metal-containing product is also neglected. As such, the results are at best of semiquantitative interest. In contrast to the ion−molecule collision experiments of Tonkyn and

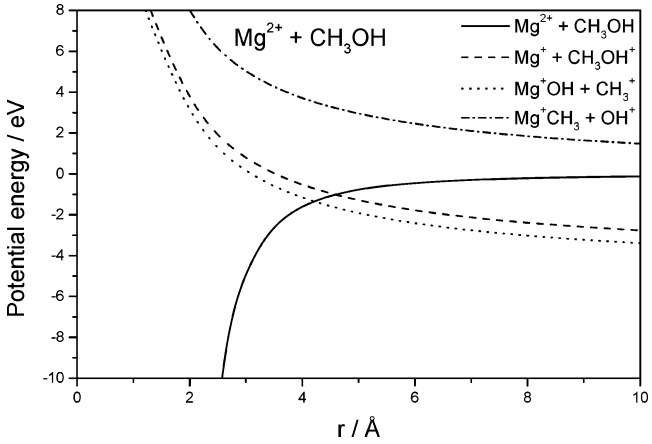

Figure 2. Calculated potential energy curves for $Mg^{2+} + CH_3OH$, showing the attractive ion−dipole and −induced dipole curve and the repulsive Coulomb curves corresponding to the appearance of different charge separation products.

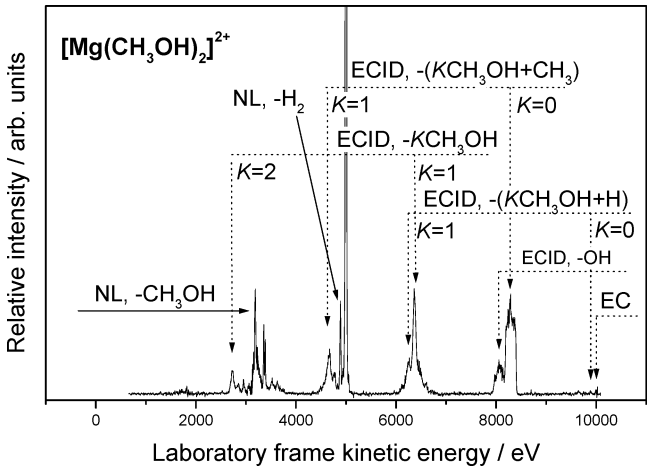

Figure 3. MIKE spectrum of $[Mg(CH_3OH)_2]^{2+}$ following collisional activation with nitrogen. NL denotes neutral loss; ECID denotes electron capture-induced dissociation; and EC denotes electron capture.

Weisshaar,[22] the methanol/dication complexes start from inside the potential well and move outward along the reaction coordinate. From the plot it can be seen that the first curve crossing to be encountered correlates with $MgOH^+$ and CH_3^+ as the reaction products. Slightly higher in energy is the curve crossing that correlates with the electron-transfer products Mg^+ and CH_3OH^+, which are not seen as the result of metastable decay. Finally, $MgCH_3^+$ and OH^+ are also not observed as charge separation products (see below) because, as Figure 2 shows, the step leading to their appearance is much higher in energy than either of the other two pathways. The reaction path calculated to have the lowest crossing energy matches the experimentally observed fragments from $[Mg(CH_3OH)_2]^{2+}$ as shown in Figure 1.

The measured width (full-width at half-maximum, fwhm) of the metastable charge separation peak in Figure 1 is 219 eV, which corresponds to a center-of-mass kinetic energy release of 2.12 eV. Using the equation $T = 14.39/r$,[15] the distance at the point of charge separation is calculated to be 6.79 Å, which is considerably longer than the crossing point of 4.21 Å shown in Figure 2. If the point of charge separation is equated with a salt bridge structure of the type proposed by Beyer et al.[23] and Beyer and Metz,[24] then this distance is also shorter than that calculated above. However, because of the possibility of internal excitation, the measured kinetic energy release has to be considered as a lower limit to the energy available, and, therefore, the calculated crossing distance for charge separation has to be an upper limit. Further discussion of this aspect of the results is given below. An interesting comparison can be made with the recent calculations of El-Nahas et al.[25] on the structure and stability of the complex $[MgCH_3OH]^{2+}$. They identified three exothermic reaction pathways each involving charge transfer, and of these the one leading to $MgOH^+ + CH_3^+$ as products had the lowest energy transition state (or curve crossing point) at all levels of theory, but in one case was not predicted to be the most exothermic pathway.[25]

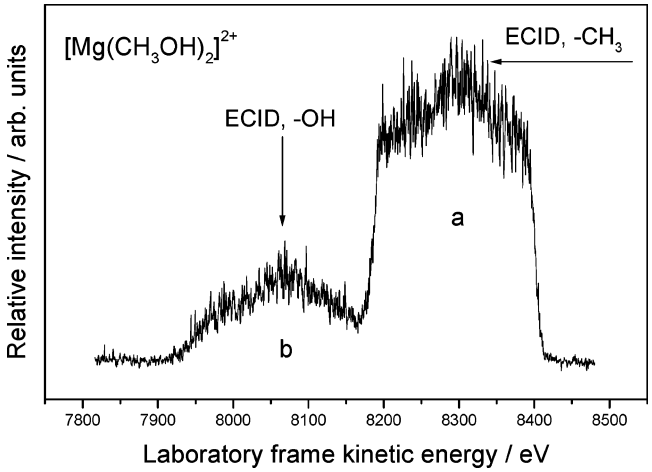

Figure 4. Expanded section of Figure 3, highlighting the products of electron capture and Coulomb explosion.

Figure 3 shows a MIKES scan recorded following the collisional activation of $[Mg(CH_3OH)_2]^{2+}$ and where the appearance of reaction products is dominated by processes that are believed to be driven by electron capture. In general, collisional activation of the smaller $[Mg(CH_3OH)_N]^{2+}$ complexes led to the observation of reactions 3−7 together with the following process:

$$[Mg(CH_3OH)_N]^{2+} + Cg \rightarrow [MgCH_2O(CH_3OH)_{N-1}]^{2+} + 2H(H_2) + Cg \quad (9)$$

Specific only to $[Mg(CH_3OH)_2]^{2+}$ is the reaction:

$$[Mg(CH_3OH)_2]^{2+} + Cg \rightarrow MgCH_3^+(CH_3OH) + OH + Cg^+ \quad (10)$$

The presence of reaction 3 in the MIKES scan of $[Mg(CH_3OH)_2]^{2+}$ would suggest that, despite being absent in the mass spectra, $[Mg(CH_3OH)]^{2+}$ can be formed as a metastable species. The latter conclusion is based on the observation that $[Mg(CH_3OH)_2]^{2+}$ and (see below) $[Mg(CH_3OH)_3]^{2+}$ exhibit metastability.

Figure 4 shows an expanded view of Figure 3 covering the same kinetic energy range (7900−8500 eV) as that given in Figure 1, but recorded in the presence of a collision gas. When compared to Figure 1, the new feature appearing at the center of peak a corresponds to the same metal-containing ionic product seen from metastable decay ($MgOH^+(CH_3OH)$ from reaction 8), but this time arising from ECID. Peak b corresponds to the product $MgCH_3^+(CH_3OH)$ and is again due to ECID. Interestingly, the latter fragment only appears when the excess energy in the precursor ion is high (from collisional activation), which, as far as the metal-containing component is concerned, would support the ordering of the potential energy curves shown in Figure 2. Likewise, the calculations of El-Nahas et al.[25] also show $MgCH_3^+$ to be a high-energy reaction product. The

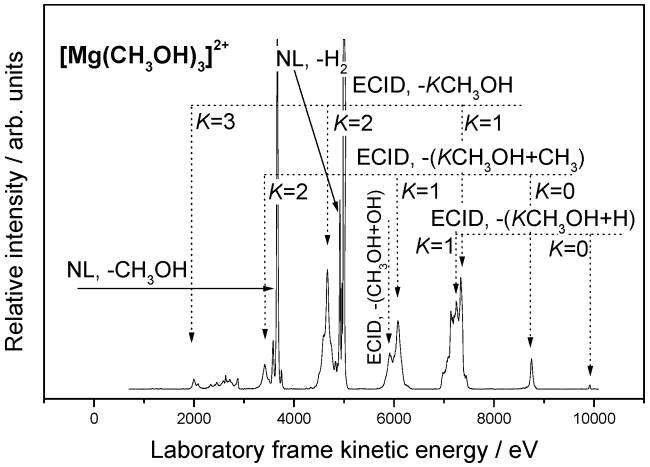

Figure 5. MIKE spectrum of $[Mg(CH_3OH)_3]^{2+}$ following collisional activation with nitrogen.

product ions MOH^+ and $MOH^+(CH_3OH)$ (M = Co and Mn) reported by Leary and co-workers are the result of heterolytic cleavage of the C−O bond,[6] as confirmed by the observation of CH_3^+ in their mass spectra. These observations contrast with the results shown here where ECID followed by the loss of neutral CH_3 or OH accounts for the distinct absence of complementary nonmetallic ions in the MIKES scans. This difference is believed to be due primarily to the much higher ion kinetic energy used in the current experiments and where the electron capture cross section is known to be comparatively large.[18]

Figure 5 shows a MIKES scan recorded following the collisional activation of $[Mg(CH_3OH)_3]^{2+}$ with nitrogen as a collision gas. $[Mg(CH_3OH)_3]^{2+}$ shows a series of neutral ligand loss, H_2 loss, and ECID processes similar to those seen for $[Mg(CH_3OH)_2]^{2+}$, with the only exception being the broad peak seen in the region 6900−7500 eV. Figure 6 shows two further MIKES scans of this region recorded with and without the presence of a collision gas. For the latter, the observation of a broad dish-shaped peak (profile A) confirms the occurrence of metastable charge separation in the form of:

$$[Mg(CH_3OH)_3]^{2+} \rightarrow MgOCH_3^+(CH_3OH) + CH_3OH_2^+ \quad (11)$$

This metastable reaction is very different from that observed for $[Mg(CH_3OH)_2]^{2+}$, and it is quite possible that the pathway changes for geometric as well as energetic reasons. A mechanism for the formation of $MgOCH_3^+(CH_3OH)$ from $[Mg(CH_3OH)_3]^{2+}$ via metastable charge separation (reaction 11) can be understood in terms of proton transfer between methanol ligands, and to help in the interpretation of this process it is useful to refer to the structures of singly charged clusters as no data are available for doubly charged species. As noted earlier, calculations by Ohashi et al.[11] show that $Mg^+(CH_3OH)_3$ clusters can adopt two separate stable structures, one where all three molecules are bound to the central metal cation, and a second where one molecule is in an outer shell hydrogen bonded to two inner shell molecules bound to the metal cation. If $[Mg(CH_3OH)_3]^{2+}$ were to adopt a similar (2 + 1) structure, either by promoting a molecule from the primary shell or via evaporation from a larger structure, then it would present an ideal geometry from which proton transfer to give $CH_3OH_2^+$ could proceed. What is particularly interesting is that this dissociation channel is very different from that seen for $[Mg(CH_3OH)_2]^{2+}$, which suggests that a similar (1 + 1) structure is not energetically accessible. Contributing factors to this change in behavior must be the gradual decline in binding energy experienced by ligands as a function of the number coordinated to a metal dication and an increase in ligand−ligand repulsion as *N* increases. A number of calculations on a range of metal dication complexes with water and methanol show that proton abstraction to form either the MOH^+ or the MOR^+ unit is preceded by the promotion of a molecule from the primary to the secondary solvation shell.[23,24,26]

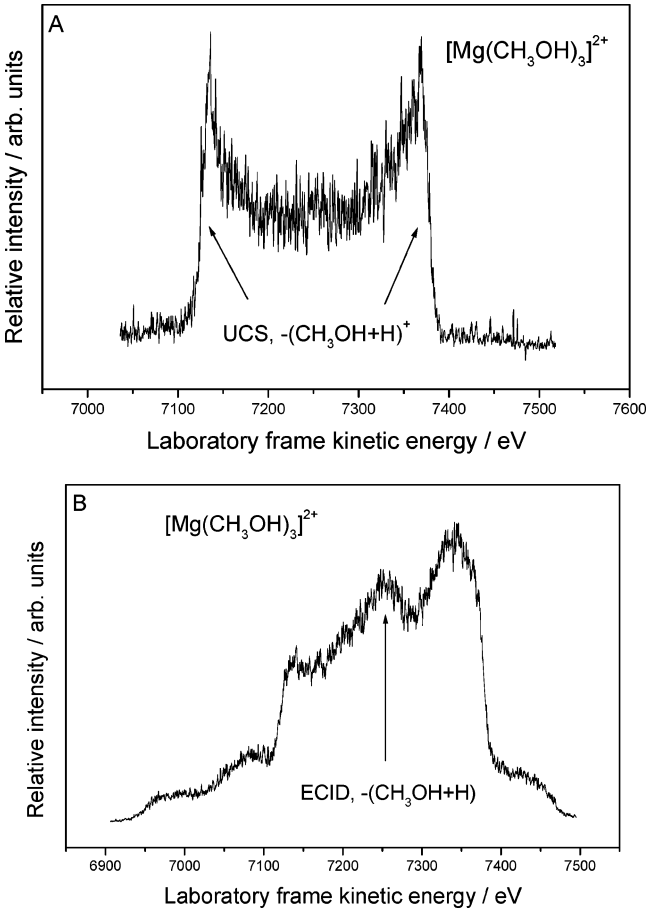

Figure 6. Kinetic energy profiles from an expanded section of the MIKES scan for $[Mg(CH_3OH)_3]^{2+}$. (A) Unimolecular metastable charge separation to produce $MgOCH_3^+CH_3OH + CH_3OH_2^+$, and (B) the same region, but following collisional activation with nitrogen.

With the introduction of a collision gas a new feature, shown in Figure 6B, appears at the center of the profile and corresponds to the same metal-containing product ion, $MgOCH_3^+(CH_3OH)$, as seen from reaction 11, but this time is believed to be formed as a result of ECID, as evidenced by the narrow spread of kinetic energy. Further experiments that involved floating the collision cell at a fixed voltage confirm the other narrow peak appearing at ∼7341 eV in Figure 6B as being due to the appearance of $[Mg(CH_3OH)_2]^+$ via ECID (reaction 5, $K = 1$).[21] A final reaction of interest is responsible for one of a pair of peaks seen at ∼6000 eV in Figure 5. The right-hand peak arises from reaction 6 with $K = 1$, but the peak to the left is due to reaction 10, which was originally designated as being specific only to the dication $[Mg(CH_3OH)_2]^{2+}$. However, close inspection of the position of the peak reveals that the reaction in $[Mg(CH_3OH)_3]^{2+}$ only proceeds when accompanied by the loss of one molecule of methanol. It would appear that the route to the formation of $MgCH_3^+(CH_3OH)$ is either facile and/or the product is unexpectedly stable. Based upon values for the bond energies of $MgOH^+$ (349 kJ

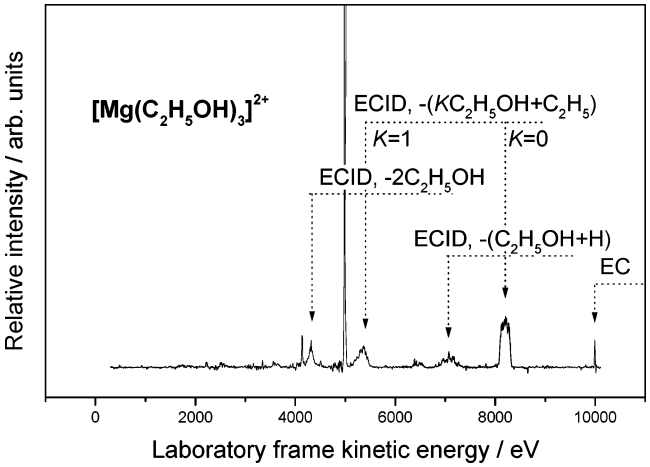

Figure 7. MIKE spectrum of $[Mg(C_2H_5OH)_3]^{2+}$ recorded following collisional activation with oxygen.

mol^{-1}) and $MgCH_3^+$ (186 kJ mol^{-1}),[27] it is not immediately obvious why reactions 6 and 10 should be in competition. Further experiments on $[Mg(CH_3OH)_4]^{2+}$ and $[Mg(CH_3OH)_5]^{2+}$ showed these larger ions to be stable with respect to Coulomb explosion and that the dominant charge reduction processes involve ECID.

None of the MIKES scans recorded for $[Mg(CH_3OH)_N]^{2+}$ complexes or indeed for most of the other $[Mg(ROH)_N]^{2+}$ complexes (see below) showed evidence of a condensation process of the type observed by Selegue and Lisy,[28] and Zhang and Castleman,[29] for alkali metal cations in association with methanol. However, two complexes, $[Mg(CH_3OH)_2]^{2+}$ and $[Mg(CH_3OH)_3]^{2+}$, exhibit prominent peaks corresponding to the loss of neutral H_2 (or 2H). Such a reaction has been observed previously for methanol in association with a range of metal cations, and where the proposed molecular product is CH_2O.[30]

(B) Mg^{2+}/Ethanol Complexes. Size-selected $[Mg(C_2H_5OH)_N]^{2+}$ ($N = 3-7$) cluster ions have been investigated for both metastable decay and collision-induced fragmentation, and Figure 7 shows a MIKES scan recorded following the collisional activation of $[Mg(C_2H_5OH)_3]^{2+}$ using oxygen. The collision-induced reactions were found to consist of processes 3−7 as summarized above. In that part of Figure 7 where the product $MgOH^+(C_2H_5OH)_2$ appears, the signal is both strong and unexpectedly complicated, and, to help with the interpretation of this feature, Figure 8 shows two further scans recorded with and without collision gas. The profile recorded in the absence of collision gas is again characteristic of fragments that are formed with a high relative kinetic energy and corresponds to the metastable charge separation reaction:

$$[Mg(C_2H_5OH)_3]^{2+} \rightarrow MgOH^+(C_2H_5OH)_2 + C_2H_5^+ \qquad (12)$$

The center-of-mass kinetic energy release determined from the peak width is 1.91 eV, which is slightly less than that measured for either $[Mg(CH_3OH)_2]^{2+}$ (2.12 eV) or $[Mg(CH_3OH)_3]^{2+}$ (2.07 eV), which is not too unexpected as molecules with larger numbers of degrees of freedom may retain more energy as internal vibrational excitation. Similar to $[Mg(CH_3OH)_N]^{2+}$, a one-dimensional potential energy curve model has been calculated and shows the reaction leading to $MgOH^+(C_2H_5OH)_2$ and $C_2H_5^+$ as being the curve crossing processes with the lowest energy barrier, which again matches the experimental result shown in Figure 8. What is particularly interesting about the Coulomb process seen for $[Mg(C_2H_5OH)_3]^{2+}$ is that reaction 12 is very different from that observed for $[Mg(CH_3OH)_3]^{2+}$,

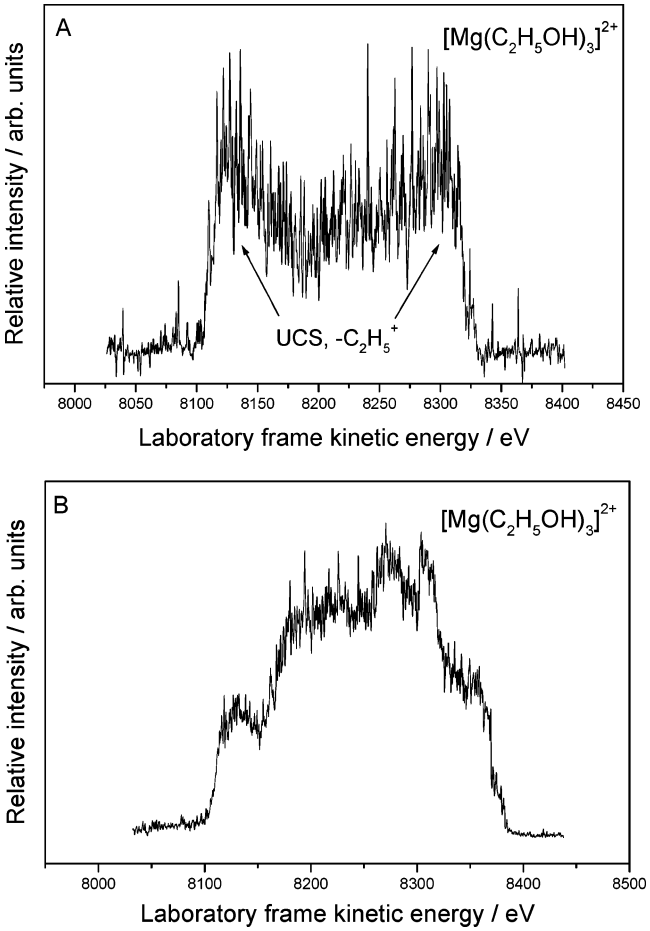

Figure 8. Kinetic energy profiles from an expanded section of the MIKES scan for $[Mg(C_2H_5OH)_3]^{2+}$. (A) Unimolecular metastable charge separation to produce $MgOH^+(C_2H_5OH)_2 + C_2H_5^+$, and (B) the same region, but following collisional activation with oxygen.

where the latter exhibited proton transfer. A further example of a switch in favored charge separation process will be presented below.

The complex structure of the profile arising from collisional activation (Figure 8B) shows the presence of a number of different processes. To simplify analysis, a potential of +963 V has been applied to the collision cell, and, as shown in Figure 9, this has the effect of separating collision-induced and metastable contributions. Peak a remains in its original position and corresponds to metastable Coulomb explosion, but with the dish-shape filled-in through collisions with gas drifting out from the collision cell. The ion at the center of the profile at ~7600 eV (peak b) corresponds to the same metal-containing product $MgOH^+(C_2H_5OH)_2$ as seen from metastable charge separation, but due to the narrow energy spread is now believed to originate from ECID. Other possible contributions to the peak are thought to include collision-induced Coulomb explosion (cf. reaction 12) and ECID processes possibly leading to the singly charged fragments $Mg^+H_2O(C_2H_5OH)_2$ and $MgO^+(C_2H_5OH)_2$. For the larger cluster ions $[Mg(C_2H_5OH)_N]^{2+}$ ($N = 4-7$), the MIKES spectra show neutral ligand loss and charge reduction reactions similar to those discussed above, but as the clusters increase in size, neutral ligand loss dominates over any form of charge reduction.

(C) Mg^{2+}/*n*-Propanol Complexes. Preliminary results from a study of $[Mg(C_3H_7OH)_N]^{2+}$ complexes by Woodward et al. demonstrated the presence of metastable charge separation.[9] This new study reveals a more complete (and complicated!) picture.

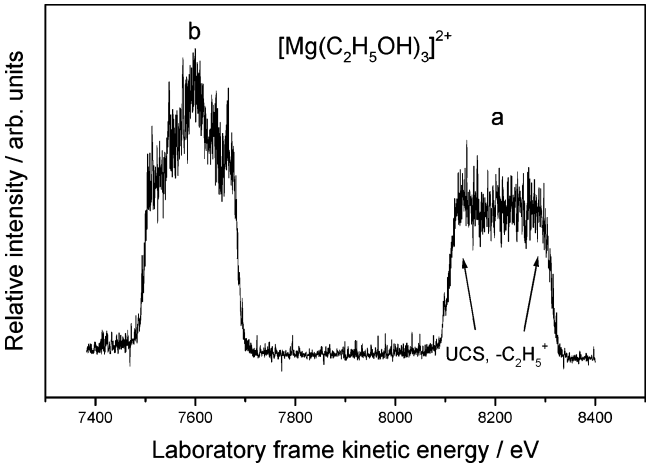

Figure 9. As for Figure 8B, but recorded with the collision cell floated at a voltage of +963 V. Peak a is predominantly formation of $MgOH^+(C_2H_5OH)_2$ from unimolecular metastable decay, and peak b includes a range of singly charged products, including $MgOH^+(C_2H_5OH)_2$, formed as a consequence of electron capture.

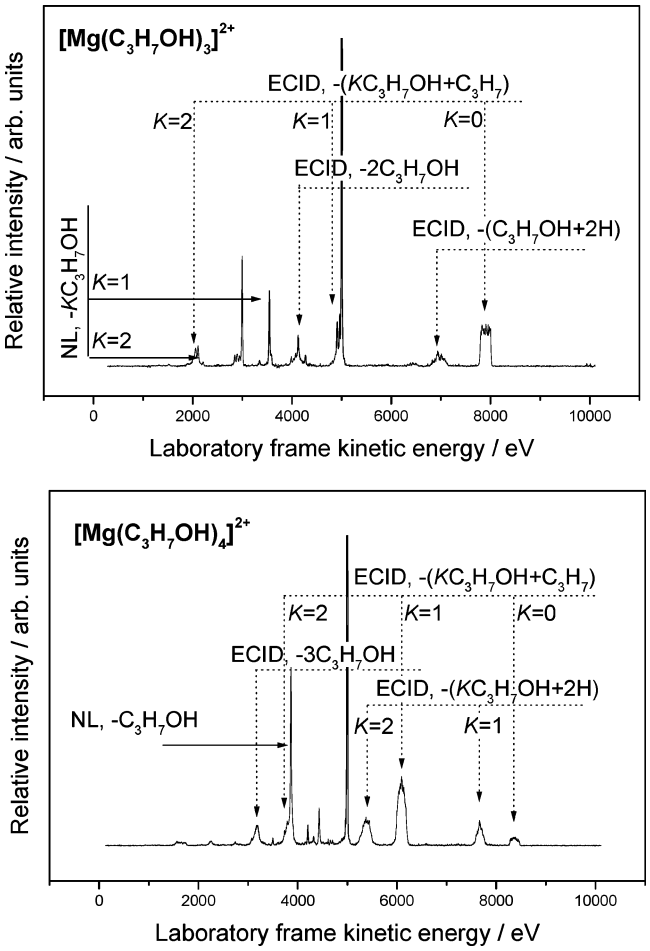

Figure 10. MIKE spectra of $[Mg(C_3H_7OH)_3]^{2+}$ and $[Mg(C_3H_7OH)_4]^{2+}$ recorded following collisional activation with oxygen.

Metastable decay and collisional excitation experiments were carried out for $[Mg(C_3H_7OH)_N]^{2+}$ ($N = 3-6$) cluster ions, and Figure 10 shows MIKES scans following the collisional activation for the ions $[Mg(C_3H_7OH)_3]^{2+}$ and $[Mg(C_3H_7OH)_4]^{2+}$ with oxygen as collision gas. Overall, the observed reaction pathways can be summarized as including contributions from steps 3, 5, 6, and 7 above together with the reaction:

$$[Mg(C_3H_7OH)_N]^{2+} + Cg \rightarrow MgOC_3H_6^+(C_3H_7OH)_{N-K-1} + KC_3H_7OH + 2H + Cg^+ \quad (13)$$

As before, the products could be H_2 and the formation of an aldehyde, but unlike reaction 9, reaction 13 is also accompanied by charge reduction. The reaction seems to be restricted to propanol and has also been seen in $[Sr(C_3H_7OH)_N]^{2+}$ complexes, but in both cases the products only appear in complexes where $N \leq 4$.[10] Again, the realization that ECID processes dominate charge transfer leads to a slightly different product assignment from those given previously for reaction 13.[9,10] Reactions equivalent to (13) have also been observed in complexes consisting of singly charged metal ions with one propanol molecule.[31]

As with previous examples, the smaller complexes show evidence of metastability, and, for this particular system, both $[Mg(C_3H_7OH)_3]^{2+}$ and $[Mg(C_3H_7OH)_4]^{2+}$ exhibit Coulomb explosion via the reaction:

$$[Mg(C_3H_7OH)_N]^{2+} \rightarrow MgOH^+(C_3H_7OH)_{N-1} + C_3H_7^+ \quad (14)$$

Charge separation is confirmed by the presence of a dish-shaped peak as shown in Figure 11 where $[Mg(C_3H_7OH)_3]^{2+}$ is the precursor ion. The measured laboratory frame kinetic energy spread of the peak (fwhm) is 225 eV, which corresponds to a center-of-mass kinetic energy release of 1.90 eV. This value is slightly larger than that recorded earlier;[9] however, the result presented here is considered to be more accurate. The analogous reaction is also seen for the next propanol complex in the series, $[Mg(C_3H_7OH)_4]^{2+}$, but this time the calculated kinetic energy release is 1.82 eV, which is consistent with the expectation that values measured for larger ions should be lower. Similar variations in kinetic energy release as a function of cluster size were also found in the study of $[Mg(NH_3)_N]^{2+}$.[16] Again, a one-dimensional potential energy curve model shows metastable charge separation to give $C_3H_7^+$ as the reaction with the lowest energy crossing point at the intersection of the two potential energy curves.

MIKES scans recorded following the collisional activation for $[Mg(C_3H_7OH)_5]^{2+}$ and $[Mg(C_3H_7OH)_6]^{2+}$ show a similar series of neutral ligand loss and charge reduction reactions,[21] except in these examples the product ion $[MgOC_3H_7(C_3H_7OH)_{N-K-1}]^+$ from the loss of KC_3H_7OH + H also begins to appear, which is a situation similar to that seen for the cluster ions $[Mg(CH_3OH)_n]^{2+}$ and $[Mg(C_2H_5OH)_n]^{2+}$.

(D) Mg^{2+}/*n*-Butanol Complexes. There have been no previous theoretical or experimental studies of $[Mg(C_4H_9OH)_N]^{2+}$ complexes. A MIKES scan of $[Mg(C_4H_9OH)_3]^{2+}$ following collisional activation with oxygen showed considerable interference below 5000 eV from ions that did not contain magnesium and could not be identified. Fortunately, most of the metallic charge reduction products were clear of this region and were found to correspond to the ions $MgOC_4H_9^+(C_4H_9OH)$ and $MgOH^+(C_4H_9OH)$. These were again attributed to electron capture-induced processes and resulted from reactions 6 and 7. The latter product was also formed as the result of metastable decay, and the profile for this is shown in Figure 12 and again has a characteristically broad profile with a center-of-mass kinetic energy release of 1.89 eV from the reaction:

$$[Mg(C_4H_9OH)_3]^{2+} \rightarrow MgOH^+(C_4H_9OH) + C_4H_9^+ \quad (15)$$

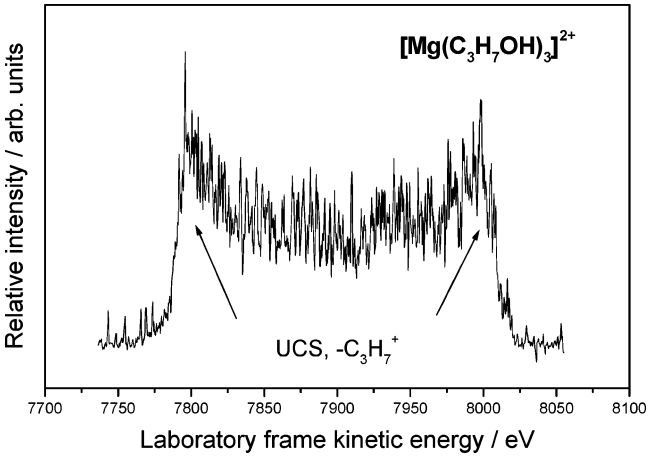

Figure 11. Kinetic energy profile recorded following the unimolecular metastable decay of $[Mg(C_3H_7OH)_3]^{2+}$ to produce $MgOH^+(C_3H_7OH)_2 + C_3H_7^+$.

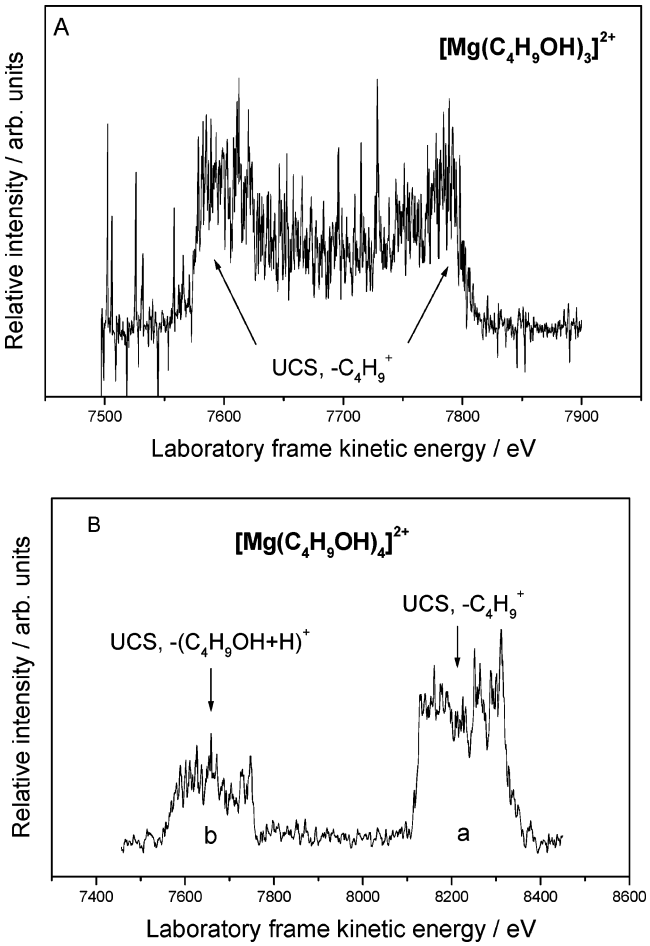

Figure 12. Kinetic energy profile recorded following: (A) the unimolecular metastable decay of $[Mg(C_4H_9OH)_3]^{2+}$ to produce $MgOH^+(C_4H_9OH)_2 + C_4H_9^+$; and (B) the unimolecular metastable decay of $[Mg(C_4H_9OH)_4]^{2+}$ to produce $MgOH^+(C_4H_9OH)_3 + C_4H_9^+$ (labeled a) and $MgOC_4H_9^+(C_4H_9OH)_2 + C_4H_9OH_2^+$ (labeled b).

A one-dimensional potential energy curve model shows metastable charge separation to form $C_4H_9^+$ as being the most energetically favorable process.

Possibly the most interesting result to emerge from these experiments with *n*-butanol is shown in Figure 12B, which presents a MIKES scan recorded for $[Mg(C_4H_9OH)_4]^{2+}$ in the absence of a collision gas. Both profiles show evidence of a large release of kinetic energy, and their positions correspond to the products $MgOH^+(C_4H_9OH)_3$) (peak a) and $MgOC_4H_9^+(C_4H_9OH)_2$ (peak b), respectively. Peak a arises from the equivalent of reaction 15, but for $N = 4$, and peak b is due to the reaction:

$$[Mg(C_4H_9OH)_4]^{2+} \rightarrow MgOC_4H_9^+(C_4H_9OH)_2 + C_4H_9OH_2^+ \quad (16)$$

This latter proton-transfer reaction was not observed for $[Mg(C_4H_9OH)_3]^{2+}$ and is not a process that, under normal circumstances, might be predicted as being energetically favorable. Furthermore, it is extremely unusual for a cluster ion to exhibit two metastable charge separation reactions because they will be in competition and will therefore be subject to a competitive shift. Because metastable decay takes place within a very narrow time window, the competitive shift imposes a very severe kinetic constraint on metastable decay and can be shown to be sensitive to energy barrier differences of just 3−4 kJ mol^{-1}.[32,33] However, one mechanism that could overcome a much larger energy difference would be if the ions under observation had different structures with, for example, the product $MgOH^+(C_4H_9OH)_3$ coming from a complex where all of the molecules are bound directly to the metal dication, and reaction 16 proceeding via a complex where one molecule occupies a hydrogen-bonded site in the second solvation shell. Because the structures being proposed for the two reaction pathways exhibited by $[Mg(C_4H_9OH)_4]^{2+}$ complexes are quite different, the constraints imposed by a competitive shift would no longer apply to metastable decay. Examples of structural differences within complexes of the same molecular composition, such as those suggested above, have been proposed in earlier work by Rodriguez-Cruz et al. on experiments with $[Mg(H_2O)_N]^{2+}$ complexes.[34,35] Again, the presence of a water molecule in the second solvation shell could be interpreted as contributing to a salt bridge structure that ultimately leads to proton abstraction and the loss of H_3O^+ or some larger solvent unit containing a proton.[23,24,26,34,35]

(E) Mg^{2+}/*t*-Butanol Complexes. A limited study has been undertaken on complexes between Mg^{2+} and *t*-butanol. It proved very difficult to generate a distribution of different sized cluster, and the only complex that could be observed with sufficient intensity for quantitative experiments was $[Mg((CH_3)_3COH)_4]^{2+}$. A MIKES scan of this ion using oxygen as the collision gas exhibited the charge reduction reactions 5−7 as shown above, and when the collision gas was removed the single metastable peak shown in Figure 13 was recorded from the reaction:

$$[Mg((CH_3)_3COH)_4]^{2+} \rightarrow MgOH^+((CH_3)_3COH)_3 + (CH_3)_3C^+ \quad (17)$$

As before, a one-dimensional potential energy curve model gives the loss of a $(CH_3)_3C^+$ group as the most favorable electron-transfer step. The measured width (fwhm) of the metastable charge separation peak in Figure 13 is approximately 200 eV, which corresponds to a center of mass kinetic energy release of 1.74 eV.

Because the observed metastability threshold occurs at $N = 4$ for $[Mg((CH_3)_3COH)_N]^{2+}$, the absence of smaller complexes in the mass spectrum is understandable. Likewise, the degree of steric hindrance experienced by additional molecules wishing to occupy sites either attached directly to the metal or hydrogen bonded in a secondary solvation shell could place an upper limit on the size of stable complex that can be generated. Given these

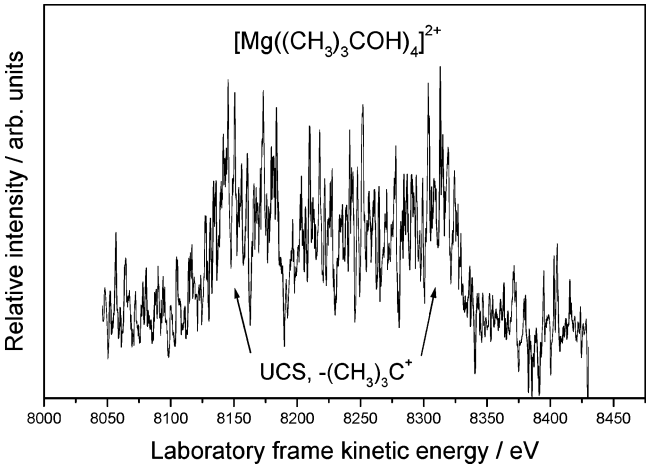

Figure 13. Kinetic energy profile recorded following the unimolecular metastable decay of $[Mg((CH_3)_3COH)_4]^{2+}$ to produce $[MgOH((CH_3)_3COH)_3]^+ + (CH_3)_3C^+$.

TABLE 1: Observed Metastable Fragmentation Pathways for $[Mg(ROH)_N]^{2+}$ Complexes

complex	metastable pathway
$[Mg(CH_3OH)_2]^{2+}$	$MgOH^+ + R^+$
$[Mg(C_2H_5OH)_3]^{2+}$	$MgOH^+ + R^+$
$[Mg(C_3H_7OH)_3]^{2+}$	$MgOH^+ + R^+$
$[Mg(C_3H_7OH)_4]^{2+}$	$MgOH^+ + R^+$
$[Mg(C_4H_9OH)_3]^{2+}$	$MgOH^+ + R^+$
$[Mg(C_4H_9OH)_4]^{2+}$	$MgOH^+ + R^+$
$[Mg((CH_3)_3COH)_4]^{2+}$	$MgOH^+ + R^+$
$[Mg(CH_3OH)_3]^{2+}$	$MgOR^+ + ROH_2^+$
$[Mg(C_4H_9OH)_4]^{2+}$	$MgOR^+ + ROH_2^+$

circumstances, it is not too surprising that $[Mg((CH_3)_3COH)_4]^{2+}$ is the only complex observed for *t*-butanol as a ligand.

Discussion

This detailed study of the metastable and collision-induced reactions of $[Mg(CH_3OH)_N]^{2+}$, $[Mg(C_2H_5OH)_N]^2$, $[Mg(C_3H_7OH)_N]^{2+}$, $[Mg(C_4H_9OH)_N]^{2+}$, and $[Mg((CH_3)_3COH)_N]^{2+}$ has revealed a wide range of charge reduction and fragmentation processes. A majority of the collision-induced processes that result in charge reduction appear to proceed via ECID and have been identified through the comparatively narrow spread in kinetic energy that accompanies fragmentation. For the most part, it has been possible to assign a generic set of ECID processes to a majority of the $[Mg(ROH)_N]^{2+}$ complexes; however, several complexes do exhibit their own distinct fragmentation patterns. Possibly the most significant result to emerge from these experiments is the observation of distinct metastable fragmentation pathways on the part of each of the different Mg^{2+}/alcohol combinations.

Two aspects of the results are worth further consideration. First is the subtle changes in metastable fragmentation pattern that have been identified for either different-sized complexes of the same alcohol (methanol) or different pathways for complexes of a single size (*n*-butanol). Table 1 summarizes these results where it can be seen that a majority of the observed metastable decay steps lead to the appearance of $MgOH^+$ as the metal-containing component to the final fragment ion, a result that is consistently supported by a simple one-dimensional curve crossing model. However, there are two fragmentation steps that follow an alternative pathway that produces $MgOR^+$ as the metal-containing fragment, but more significantly leads to the appearance of a protonated alcohol as the complementary fragment ion. Examples of where proton abstraction has been modeled in dication complexes using density functional theory always show the reaction step as being preceded by the movement of a molecule from the primary solvation shell into a hydrogen-bonded position in the second shell.[23,24,26] Even under circumstances where there are already secondary shell molecules present, this movement of a solvent molecule appears to be a prerequisite to proton abstraction.[26] Given these circumstances, it would seem reasonable to assume that similar behavior will prevail in the case of $[Mg(ROH)_N]^{2+}$ complexes and that the difference between $[Mg(CH_3OH)_2]^{2+}$ and $[Mg(CH_3OH)_3]^{2+}$ is that the latter more readily adopts a second-shell structure similar to those identified in a range of singly charged complexes.[11] In the case of $[Mg(C_4H_9OH)_4]^{2+}$, there is quite a compelling case for proposing different structures for the two separate fragmentation pathways exhibited by the ion. The competitive shift makes it extremely unlikely that an ion with a single structure will undergo two distinct metastable pathways unless they have almost identical rate constants. Therefore, it is concluded that the $MgOR^+$ product comes from $[Mg(C_4H_9OH)_4]^{2+}$ complexes that, at some stage following ionization, adopt a $(3 + 1)$ structure.

TABLE 2: Observed Metastable Switching Points, N_{cross}, for $[Mg(ROH)_N]^{2+}$ Complexes[a]

ligand	N_{cross}	IE(R)[36]/eV
CH_3OH	2,3	9.84
C_2H_5OH	3	8.12
C_3H_7OH	3,4	8.09
C_4H_9OH	3,4	8.02
$(CH_3)_3COH$	4	6.70

[a] IE(R) is the ionization energy of the radical that is produced as the complementary ion as a result of charge separation.

For two of the observed metastable decay processes, charge separation takes the form of proton transfer, and so the proton affinities (PA) of the molecules might be expected to influence the size and composition of complexes that exhibit this alternative pathway. Although there is a gradual increase in PA across the linear alcohol series, rising from methanol (754 kJ mol^{-1}) to *n*-butanol (789.2 kJ mol^{-1}),[36] that is not matched by an increased tendency to exhibit proton transfer. Indeed, the alcohol with the highest PA, *t*-butanol (802.6 kJ mol^{-1}),[36] shows no evidence of proton transfer; however, this may be for steric rather than energetic reasons. We would conclude that structure (molecular configuration) is the deciding factor in whether or not a metastable pathway involves proton transfer. Supporting evidence for this conclusion is given below.

A second significant aspect to the results is the observed variation in size of complex that undergoes metastable decay as a function of the type and number of alcohol molecules. These data are summarized in Table 2, where it can be seen that there is a gradual increase in the number of molecules required to stabilize a complex against metastable decay, and at first sight, this trend would appear to vary as a function of the size of alcohol molecule. Referring to Figure 2, it can be seen that metastability arises when the repulsive Coulomb and the attractive electrostatic potential energy curves intersect at a crossing point below the $Mg^{2+} + ROH$ asymptote. Taking the latter as a reference point, then it is clear that the lower in energy the Coulomb curve sits with respect to the attractive potential, the higher is the probability that the complex will exhibit metastable decay. This statement assumes that metastable decay is driven by a statistical process whereby some fraction of any residual internal energy eventually finds its way into a reaction coordinate that intersects with the point where the two curves cross.[37] The height of the crossing point with respect to the well

TABLE 3: Measured Kinetic Energy Releases Following the Metastable Decay of $[Mg(ROH)_N]^{2+}$ Complexes

ligand	N	KER/eV	ΔH^c/eV	$\Delta H - E_{cross}{}^d$/eV	KER (%)
CH_3OH^a	2	2.12	4.83	3.47	61
$C_2H_5OH^a$	3	1.91	6.47	3.87	49
$C_3H_7OH^a$	3	1.90	6.47	3.76	50
$C_3H_7OH^a$	4	1.82	6.47	3.76	48
$C_4H_9OH^a$	3	1.89	6.64	3.63	52
$C_4H_9OH^a$	4	1.75	6.64	3.63	48
$(CH_3)_3COH^a$	4	1.74	7.79	4	43
CH_3OH^b	3	2.07			
$C_4H_9OH^b$	4	1.29			

[a] $MgOH^+(ROH)_{N-1} + R^+$ as products. [b] $MgOR^+(ROH)_{N-2} + ROH_2^+$ as products. [c] Exothermicity with respect to the products $Mg^{2+} + ROH$. [d] Derived from potential energy curves for the step $Mg^{2+} + ROH$.

of the attractive curve that binds the complex is then taken as being representative of an activation barrier. A number of factors are going to influence the relative positions of the two curves, and several of these will be approximately equal across the range of alcohols. The solvation energy of Mg^{2+}, the ionization energy of Mg^+, and the bond energy of $MgOH^+$ are unlikely to exhibit significant variation as a function of the type of alcohol. Likewise, the ROH bond energy increases by just 0.18 eV on going from methanol to *t*-butanol. What does change significantly, and is shown in Table 2, is the ionization energy (IE) of the radical, R˙, which in the form of R^+ is, in most case, the other product of metastable decay. As can be seen, IE drops from 9.84 eV for CH_3O to 6.70 eV for the *t*-butyl radical,[36] and in doing so makes metastable decay increasingly exothermic and, therefore, more likely to have a lower activation barrier. As a result, increasing numbers of molecules are required to stabilize the different types of complex. For the linear chain alcohols larger than methanol, the decline in the ionization energy of R˙ is not as dramatic, and so the metastable threshold remains more or less constant.

Table 3 summarizes the kinetic energy releases measured for each of the metastable reactions leading to the formation of $MgOH^+(ROH)_M + R^+$. Also shown in the table is the exothermicity (ΔH) of the charge separation process, calculated with respect to the products $Mg^{2+} + ROH$ (the only system for which quantitative data are available). However, this quantity is not a good measure of the energy available for partitioning to the products of metastable decay because the point at which the two potential energy curves cross (see Figure 2) lies below the above asymptote. Again taking $Mg^{2+} + ROH$ as a reference point, the energy of the crossing point, E_{cross}, can be estimated and the difference $\Delta H - E_{cross}$ taken as being approximately equal to the energy available as kinetic energy and for partitioning to the reaction products. This quantity is also shown in Table 3 and has also been used to express the kinetic energies as a percentage of the total energy available. Also shown in Table 3 are the kinetic energy releases measured for the two proton-transfer reactions. For methanol it is not possible to make a comparison with the $MgOH^+$ channel because of differences in the size of the precursor ions. However, for the *n*-butanol complex $[Mg(C_4H_9OH)_4]^{2+}$ it can be seen that there is a significant difference in energy release between the two reaction paths identified in Figure 12b. Although the shape of a potential energy surface can have a marked influence on energy release,[38] the difference seen here could also be due, in part, to the proton-transfer channel being less exothermic. This conclusion would be consistent with the earlier assumption that proton affinity does not make a significant contribution toward determining reaction pathway.

Acknowledgment. We would like to thank EPSRC for financial support for this series of experiments and Nottingham University for providing financial support for B.W.

References and Notes

(1) Stace, A. J. *J. Phys. Chem. A* **2002**, *106*, 7993.
(2) Combariza, M. Y.; Fahey, A. M.; Milshteyn, A.; Vachet, R. W. *Int. J. Mass Spectrom.* **2005**, *244*, 109.
(3) Schroder, D.; Schwarz, H. *J. Phys. Chem. A* **1999**, *103*, 7385.
(4) Walker, N. R.; Wright, R. R.; Barran, Cox, H.; Stace, A. J. *J. Chem. Phys.* **2001**, *114*, 5562.
(5) Woodward, C. A.; Dobson, M. P.; Stace, A. J. *J. Phys. Chem. A* **1997**, *101*, 2279.
(6) Kohler, M.; Leary, J. A. *J. Am. Soc. Mass Spectrom.* **1997**, *8*, 1124.
(7) Thompson, C. J.; Faherty, K. P.; Stringer, K. L.; Metz, R. B. *Phys. Chem. Chem. Phys.* **2005**, *7*, 814.
(8) Walker, N. R.; Dobson, M.; Wright, R. R.; Barran, P. E.; Murrell, J. N.; Stace, A. J. *J. Am. Chem. Soc.* **2000**, *122*, 11138.
(9) Woodward, C. A.; Dobson, M. P.; Stace, A. J. *J. Phys. Chem.* **1996**, *100*, 5605.
(10) Dobson, M. P.; Stace, A. J. *Int. J. Mass Spectrom. Ion Processes* **1997**, *165/166*, 5.
(11) Machinaga, H.; Ohashi, K.; Inokuchi, Y.; Nishi, N.; Sekiya, H. *Chem. Phys. Lett.* **2004**, *391*, 85.
(12) Lu, W.; Yang, S. *J. Phys. Chem. A* **1998**, *102*, 825.
(13) Cabaleiro-Lago, E. M.; Rodríguez-Otero, J. *J. Phys. Chem. A* **2002**, *106*, 7195.
(14) Walker, N. R.; Wright, R.; Stace, A. J. *J. Am. Chem. Soc.* **1999**, *121*, 4837.
(15) Cooks, R. G.; Beynon, J. H.; Caprioli, R. M.; Lester, G. R. *Metastable Ions*; Elsevier: Amsterdam, 1973.
(16) Wu, B.; Duncombe, B. J.; Stace, A. J. *J. Phys. Chem. A* **2006**, *110*, 8423.
(17) Duncombe, B. J.; Duale, K.; Buchanan-Smith, A.; Stace, A. J. *J. Phys. Chem. A* **2007**, *111*, 5158.
(18) Ishii, K.; Itoh, A.; Okuno, K. *Phys. Rev. A* **2004**, *70*, 042716.
(19) Sanekata, M.; Misaizu, F.; Fuke, K.; Iwata, S.; Hashimoto, K. *J. Am. Chem. Soc.* **1995**, *117*, 747.
(20) Watanabe, H.; Iwata, S.; Hashimoto, K.; Misaizu, F.; Fuke, K. *J. Am. Chem. Soc.* **1995**, *117*, 755.
(21) Wu, B. Gas-phase studies of multiply-charged metal-ligand complexes. Ph.D. thesis, University of Nottingham, 2007.
(22) Tonkyn, R.; Wisshaar, J. C. *J. Am. Chem. Soc.* **1986**, *108*, 7128.
(23) Beyer, M. K.; Williams, E. R.; Bondybey, V. E. *J. Am. Chem. Soc.* **1999**, *121*, 1565.
(24) Beyer, M. K.; Metz, R. B. *J. Phys. Chem. A* **2003**, *107*, 1760.
(25) El-Nahas, A. M.; El-Demerdash, S. H.; El-Shereefy, E. E. *Int. J. Mass Spectrom.* **2007**, *263*, 267.
(26) Cox, H.; Stace, A. J. *J. Am. Chem. Soc.* **2004**, *125*, 233.
(27) *Organometallic Ion Chemistry*; Freiser, B. S., Ed.; Kluwer: Dordrecht, The Netherlands, 1996; p 283.
(28) Selegue, T. J.; Lisy, J. M. *J. Am. Chem. Soc.* **1994**, *116*, 4874.
(29) Zhang, X.; Castleman, A. W., Jr. *J. Am. Chem. Soc.* **1992**, *114*, 8607.
(30) Huang, S.; Holman, R. W.; Gross, M. L. *Organometallics* **1986**, *5*, 1857.
(31) Karrass, S.; Prüsse, T.; Eller, K.; Schwarz, H. *J. Am. Chem. Soc.* **1989**, *111*, 9018.
(32) Stace, A. J.; Shukla, A. K. *J. Am. Chem. Soc.* **1982**, *104*, 5314.
(33) Stace, A. J.; Moore, C. *J. Am. Chem. Soc.* **1983**, *105*, 1814.
(34) Rodriguez-Cruz, S. E.; Jockusch, R. A.; Williams, E. R. *J. Am. Chem. Soc.* **1999**, *121*, 1986.
(35) Rodriguez-Cruz, S. E.; Jockusch, R. A.; Williams, E. R. *J. Am. Chem. Soc.* **1999**, *121*, 8898.
(36) http://webbook.nist.gov/chemistry/.
(37) Harvey, J. N. *Phys. Chem. Chem. Phys.* **2007**, *9*, 331.
(38) Levine, R. D.; Bernstein, R. B. *Molecular Reaction Dynamics and Chemical Reactivity*; OUP: Oxford, 1987.